

# **Aqueous Cation-Amide Binding: Free Energies and IR Spectral Signatures by Ab Initio Molecular Dynamics**

*Eva Pluhařová<sup>1</sup>, Marcel D. Baer,<sup>2</sup> Christopher J. Mundy,<sup>2</sup> Burkhard Schmidt,<sup>3</sup> and Pavel Jungwirth<sup>1\*</sup>*

<sup>1</sup>Institute of Organic Chemistry and Biochemistry, Academy of Sciences of the Czech Republic, Flemingovo nam. 2, 16610 Prague 6, Czech Republic

<sup>2</sup>Physical Sciences Division, Pacific Northwest National Laboratory, Richland, WA 99352, USA

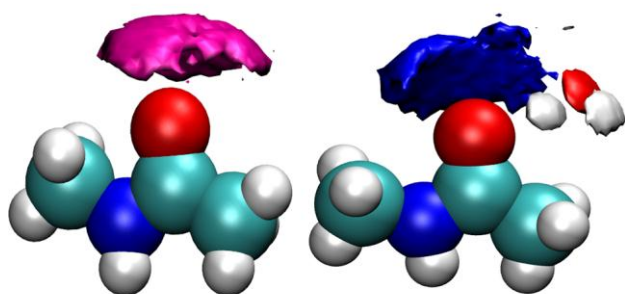
<sup>3</sup>Institut für Mathematik, Freie Universität Berlin, Arnimallee 6, D-14195 Berlin, Germany

*\*Corresponding author: [pavel.jungwirth@uochb.cas.cz](mailto:pavel.jungwirth@uochb.cas.cz)*

## ABSTRACT

Understanding specific ion effects on proteins remains a considerable challenge. N-methylacetamide serves as a useful proxy for the protein backbone that can be well characterized both experimentally and theoretically. The spectroscopic signatures in the amide I band reflecting the strength of the interaction of alkali cations and alkali earth dications with the carbonyl group remain difficult to assign and controversial to interpret. Herein, we directly compute the IR shifts corresponding to the binding of either sodium or calcium to aqueous N-methylacetamide using *ab initio* molecular dynamics simulations. We show that the two cations interact with aqueous N-methylacetamide with different affinities and in different geometries. Since sodium exhibits a weak interaction with the carbonyl group, the resulting amide I band is similar to an unperturbed carbonyl group undergoing aqueous solvation. In contrast, the stronger calcium binding results in a clear IR shift with respect to N-methylacetamide in pure water.

## TOC GRAPHIC



**KEYWORDS:** sodium, calcium, N-methylacetamide, peptide bond, umbrella sampling.

Interaction of ions with the protein backbone is of general interest in protein chemistry, primarily in terms of understanding stabilizing and destabilizing (denaturing) effects of salts<sup>1-6</sup>. Although an important role of amino acid side chains is being increasingly recognized<sup>7-9</sup>, the backbone remains one of the key players in ion specific effects on proteins. For anions, there is a general consensus that large soft ones (I<sup>-</sup>, SCN<sup>-</sup>, ClO<sub>4</sub><sup>-</sup>, *etc.*) bind to the backbone, while small hard ones (F<sup>-</sup>, SO<sub>4</sub><sup>2-</sup>, *etc.*) do not<sup>1, 4, 5</sup>. However, for cations, the situation is less clear. Partitioning models assume an appreciable interaction of hard cations like Ca<sup>2+</sup>, Li<sup>+</sup>, or Na<sup>+</sup> with the backbone<sup>10</sup>. However, as we showed recently<sup>11</sup>, this assumption is partially based on old measurements for peptides with supposedly capped termini, where the C-terminus was actually uncapped<sup>1</sup>, which changes interpretation of the data. Also, the recently measured amide I IR signals are interpreted in terms of very weak (actually none for Na<sup>+</sup>) cationic interactions<sup>12</sup>, while classical molecular dynamics (MD) simulations indicate some, albeit weak, binding of sodium to the peptide bond<sup>13, 14</sup>.

Classical MD simulations provide valuable insight into ion pairing, however, the results may be sensitive to the particular choice of interaction parameters<sup>15</sup>. There is, therefore, need to explore ion binding to the peptide bond in bulk water using electronic structure methods, which should be more accurate and less biased than empirical force fields in description of the heterogeneous environment in the vicinity of a protein. Indeed, we have shown recently, that accurate description of ion pairing in bulk water can be achieved by *ab initio* molecular dynamics (AIMD)<sup>16</sup>. AIMD, based on the density functional theory (DFT), can not only provide a reliable potential of mean force for ion pairing<sup>16</sup>, but can naturally describe the vibrational fingerprint of molecules that can be directly mapped to an IR spectrum<sup>17</sup>. Thus, the relatively unbiased representation of the interaction afforded by DFT is well suited to provide additional perspective regarding the strength of cationic binding to the peptide bond.

As a suitable proxy to model interactions at the protein backbone we employ N-methylacetamide (NMA) as one of the simplest molecules containing the peptide bond<sup>1, 18</sup>. Herein, we use AIMD to construct the free energy profiles for binding calcium and sodium to aqueous NMA and model the concomitant changes in the amide I spectral signatures. Our results suggest that  $\text{Ca}^{2+}$  and  $\text{Na}^+$  interact with the carbonyl group with different strengths and at different geometries leading to a measurable IR signature for calcium, but a much weaker one for sodium. Thus, the present calculations produce a microscopic picture of specific ion effect regarding cation binding to a model protein backbone.

Before starting computationally demanding AIMD free energy calculations of  $\text{Ca}^{2+}$  or  $\text{Na}^+$  binding to aqueous NMA, we found it useful to run 50 ps of direct AIMD simulation for each of these two systems, as well as for NMA in neat water. Calcium stayed bound to the carbonyl group for the entire trajectory at a distance of 2.3 - 2.4 Å from the carbonyl oxygen. Sodium was also found to be bound to the carbonyl oxygen with a mean distance of about 2.4 Å. However, the distribution of sampled distances for the  $\text{Na}^+$  was significantly broader than for  $\text{Ca}^{2+}$  suggesting a weaker binding for the former cation. These differences can be captured visually by plotting the cationic nuclear densities around NMA as shown in Figure 1. Despite the considerable width of the distributions, it is clearly visible that calcium binds to the carbonyl preferentially in a collinear fashion, directly replacing about two water molecules. In contrast, the sodium distribution is skewed with respect to the C=O axis. Consequently, sodium effectively replaces only a single water molecule, which provides a structural rationalization for its weaker binding to the carbonyl group compared to calcium. For comparison, we also show in Figure 1 the distribution of water molecules around NMA in pure water. As will be discussed more quantitatively below ( Figure 4b) we see on average that about two water molecules are hydrogen bonded to the C=O group (out of which sodium replaces one and calcium both when salt is added).

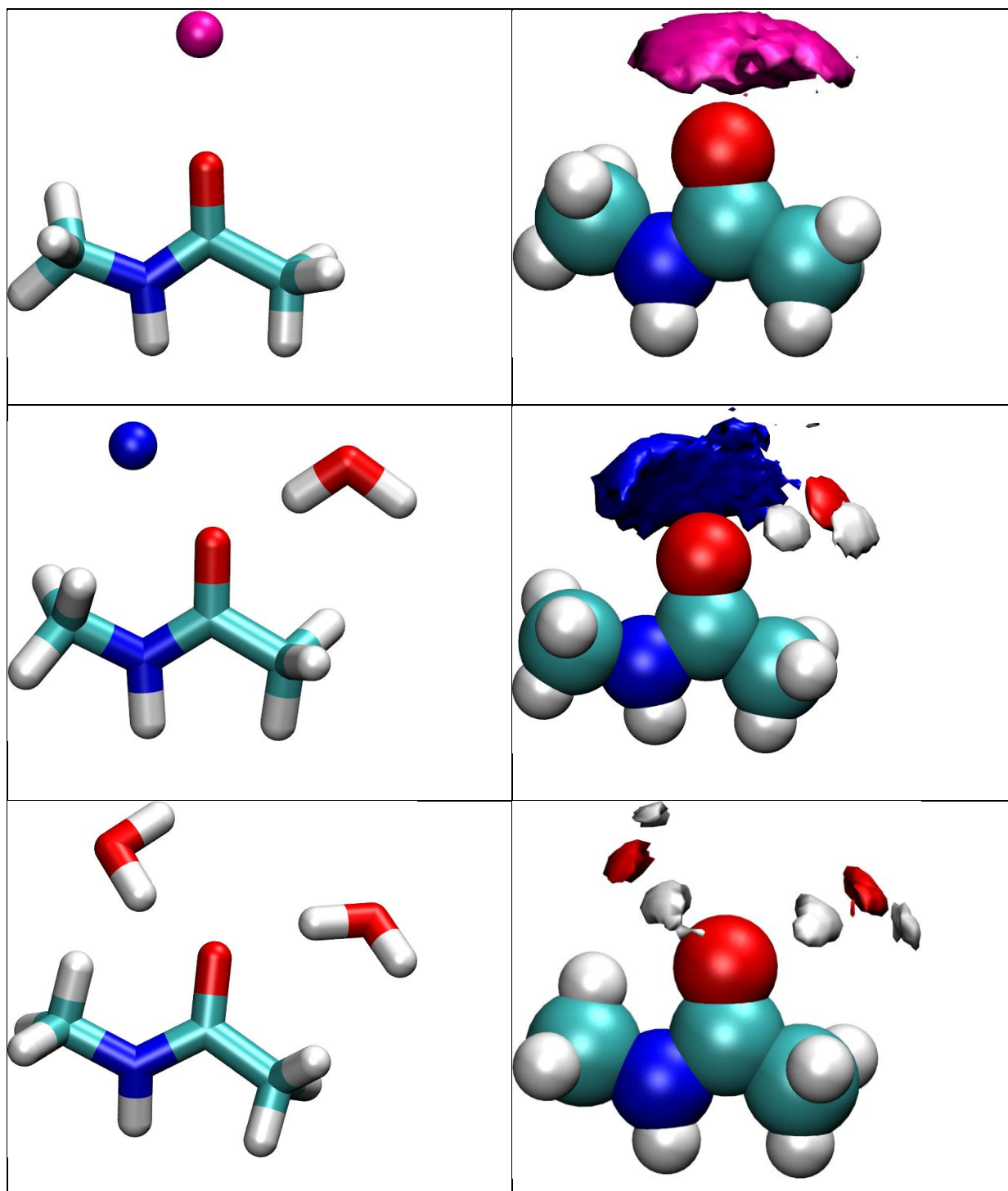


**Figure 1:** Representative snapshots (left) and density maps (right) of i) top:  $\text{Ca}^{2+}$  (magenta), ii) middle:  $\text{Na}^+$  (blue) and water oxygen (red) and hydrogen (white), iii) bottom: water oxygen (red) and hydrogen (white) for salt-free system, in all cases around the carbonyl group of aqueous N-methylacetamide.

A detailed and quantitative way to characterize ion binding to the peptide bond in water is to calculate the corresponding free energy profile. To this end, we employ AIMD in conjunction with umbrella sampling and the weighted histogram analysis<sup>19</sup>. In principle, three

coordinates are needed to fully describe the position of the cation with respect to the NMA molecule, namely the two  $\text{C}=\text{O}\cdots\text{cation}$  angular coordinates as functions of the  $\text{O}\cdots\text{cation}$  distance. It is, however, technically not feasible to sample the whole distribution given the necessarily limited timespan of the AIMD simulations. Nevertheless, as a self-consistent check we were able to determine the effect of limited angular sampling on the shape of the free energy profile from classical simulations employing an empirical force field and show that it is very small, see Supporting Information (SI). For these auxiliary classical MD simulations, used also for generating initial conditions of umbrella sampling simulations, we selected the OPLS force field<sup>20</sup>, as it gives the closest agreement with AIMD for the position of the first minimum for cationic binding to the carbonyl group to NMA (for details see SI).

The resulting AIMD free energy profiles for calcium and sodium binding to the carbonyl group of NMA in water are presented in Figure 2. The contact minimum for  $\text{C}=\text{O}\cdots\text{Ca}^{2+}$  binding is located at 2.35 Å. The corresponding solvent shared structure situated at 4.2 Å lies ~3 kJ/mol above the contact ion minimum. Unlike in the calcium case, similar analysis for the sodium ion assigns the lower minimum to the solvent-shared one at 4.8 Å, lying ~5 kJ/mol below the contact minimum at 2.4 Å. The differences between the calcium and sodium are also seen when examining the transition state (TS) going from the global to the local minimum. For calcium the TS is located at a separation of 3.1 Å with a barrier with respect to the contact minimum of 14 kJ/mol. For sodium, the TS is located at 3.1 Å with a barrier of 12 kJ/mol with respect to the solvent shared minimum. Within our calculations it is hard to establish accurately the relative stability of the above observed minima with respect to the infinitely separated pair. Even though it is safe to conjecture that the free energy for binding does not change much at distances beyond the solvent shared minimum (*i.e.*, >6 Å) the difficult nature of these calculations makes this hard to fully quantify. Nevertheless, as we show below, the interpretation of the experimental IR spectrum does not rely on making a definitive

statement regarding the relative binding energies referenced to the bulk. All that is needed to interpret the experiment is the sampling in the bound state of both ions.

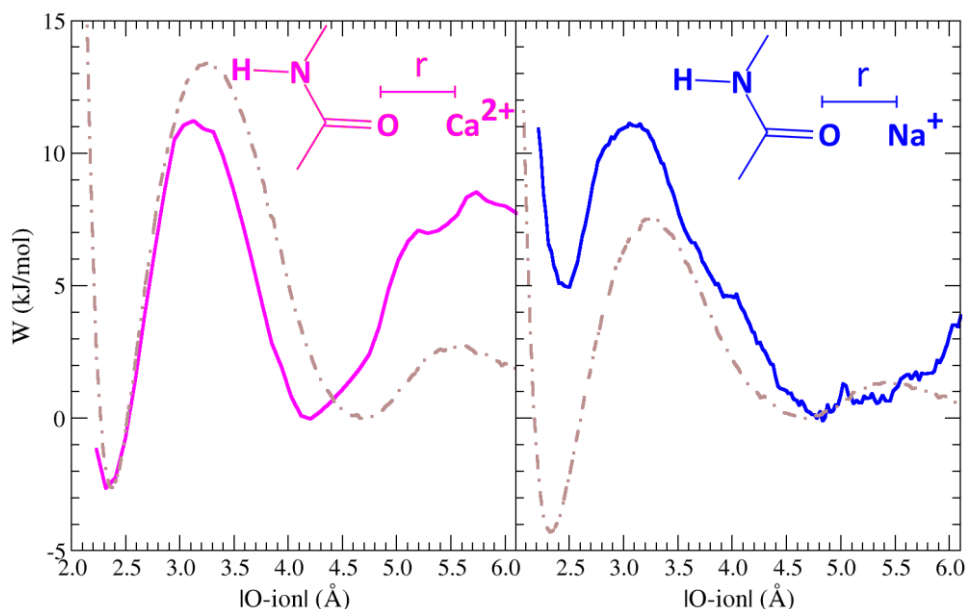


**Figure 2:** Free energy profile for CO...cation dissociation obtained by umbrella sampling combined with DFT-based AIMD (colored lines) or force field MD (brown dot-dashed lines). All profiles are corrected by the volume entropy factor of  $2 \cdot k_B \cdot T \cdot \ln(r/r_0)$ . The free energy of the solvent shared state minimum is set to zero in all cases.

A direct comparison of the AIMD free energy profiles of  $\text{Na}^+$  and  $\text{Ca}^{2+}$  binding to NMA to those obtained using classical interaction potentials reveals significant quantitative differences (for detailed discussions see SI). These differences concern both the absolute and relative stabilities of the contact and solvent-shared minima, as well as the barrier height between them (see Figure 2 and SI). In particular, positions of these stationary points differ by as much as  $0.5 \text{ \AA}$  and the relative stabilities of the two minima vary by up to 3 kJ/mol. Moreover, unlike AIMD all the present force field calculations place the contact minimum below the solvent-shared one.

Having access to the dynamics we are afforded a complete picture of the IR spectra through the time correlations of the dipole moments of all the molecular species. It was shown in earlier work that the solvent induced blue-shift of the carbonyl stretch for NMA is well reproduced with density functionals based on the generalized gradient approximation and a clear spectral assignment can be made<sup>21, 22</sup>. The influence of a formed NMA-cation contact pair on the carbonyl stretch frequency within the amide-I band vibrational spectra can be quantitatively determined through the comparison of the calculated IR spectra for free aqueous NMA and NMA with a cation ( $\text{Ca}^{2+}$  or  $\text{Na}^+$ ) in an equilibrium position of a contact pair. To make a more direct contact with experimental conditions the coupling between the water bend and the carbonyl stretch are suppressed by replacing all acidic protons (*i.e.* those of water and amide) by deuterium.

The change of the carbonyl stretch frequency upon contact pair formation can be predicted by calculating the IR absorption spectra using either maximally localized Wannier functions or the power spectra of the C=O bond length<sup>21-24</sup>. Comparing the IR-spectra and power spectra and unambiguous assignment of the C=O stretch is easily achieved. The free aqueous NMA shows a broad absorption peaking around  $1570\text{ cm}^{-1}$  (Figure 3) which compares reasonably well with the experimental values<sup>25, 26</sup> of  $1620\text{-}1640\text{ cm}^{-1}$ . Previous DFT-based studies have shown similar deviations from experiment, albeit typically of opposite sign, which could be traced to different functionals and simulation protocol<sup>26, 27</sup>.

Further refinement of our analysis is performed for the free NMA simulations by sorting the individual trajectories into distinct hydrogen bonding patterns around the amide group. By counting water hydrogens within  $2.25\text{ \AA}$  of the carbonyl oxygen and oxygens within  $2.25\text{ \AA}$  of the amide proton, three distinct structures can be identified as shown in Figure 4. Selecting trajectories based on this criteria and calculating the subsequent spectra for the subsets of structures suggests a picture where the ensemble averaged simulation of the free NMA covers a



broad spectrum spanning characteristic frequencies from  $1550\text{ cm}^{-1}$  to  $1570\text{ cm}^{-1}$ . Similar analysis can be performed also for the simulations containing the ions in the contact cation-NMA geometry.

Interestingly, for the case of  $\text{Na}^+$ , the ensemble averaged spectrum ((a.1) and a.2) in Figure 3) *does not* show a significant shift in the carbonyl stretch relative to the free aqueous NMA that might be anticipated based on the close proximity of a cation. Thus, our simulations suggest that although the  $\text{Na}^+$  can be present as a contact ion-pair with the carbonyl group, it may not be detectable via IR spectroscopy of the carbonyl group. Moreover, two distinct structural motifs are found for the  $\text{NMA--Na}^+$  contact ion pair, namely with either one or two water hydrogen bonds to the carbonyl oxygen (see Figure 4 b)).

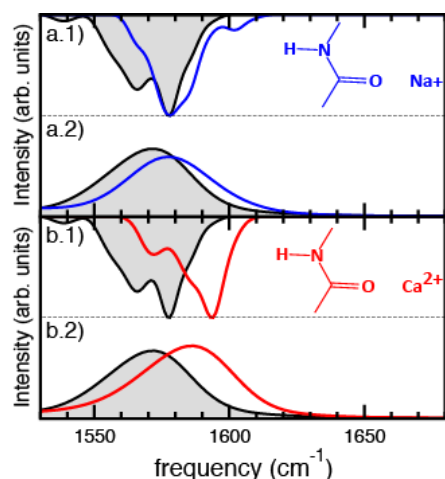


**Figure 3:** Comparison of the ensemble averaged free aqueous NMA C=O bond length power spectrum (grey with black outline) compared to the  $\text{Na}^+$  (blue) and  $\text{Ca}^{2+}$  (red) contact pair in a.1) and b.1), respectively. a.2) and b.2) show the ensemble averaged IR-absorption spectra based on the autocorrelation of the molecular dipole as described in the method section for the free aqueous NMA (black),  $\text{Na}^+$  (blue) and  $\text{Ca}^{2+}$  (red) contact pairs.

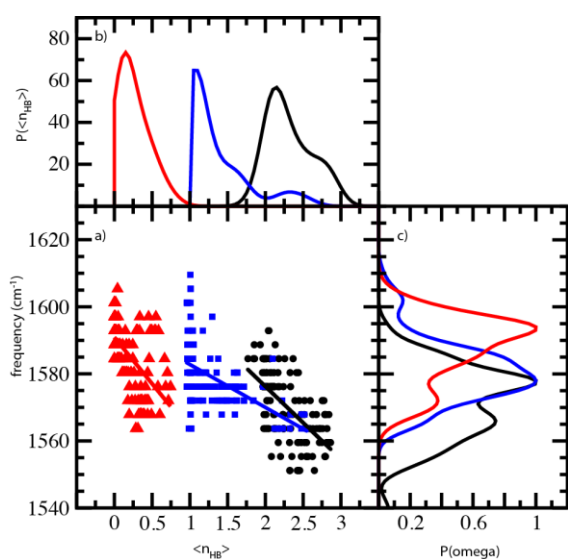


**Figure 4:** Correlation of the most probably frequency in the spectral range between  $1500 \text{ cm}^{-1}$  and  $1700 \text{ cm}^{-1}$  versus average hydrogen bond number  $\langle n_{\text{HB}} \rangle$  using 4ps windows is shown in a). The symbols represent the frequency for each individual run based on the trajectories for the free aqueous NMA (black),  $\text{Na}^+$  (blue) and  $\text{Ca}^{2+}$  (red) contact pairs, the straight lines represent linear fits to the data. Figure b) shows the probability distribution of the average hydrogen bonded number and c) the frequency distribution, in which the maximum is set to 1 for better comparison.

For  $\text{Ca}^{2+}$  a very different picture emerges ((b.1) and b.2) in Figure 3). Here, the spectrum of the contact NMA-- $\text{Ca}^{2+}$  pair is clearly blue shifted by about  $23 \text{ cm}^{-1}$  with respect to that of the free aqueous NMA in a very good agreement with the experimentally observed spectra<sup>12</sup>. Interestingly, the sign of the shift is opposite to the red shift that has been argued in a previous computational work fitting the amide I band in the presence of an electric field.<sup>28</sup> Our work, however, focuses on the shift of the amide I band in the presence of an ion and the concomitant change in hydrogen bond patterns. Thus, we may tentatively argue that the blue shift we observe in agreement with experiment<sup>12</sup> is due to less hydrogen bonding in the presence of  $\text{Ca}^{2+}$ . This spectral feature is experimentally realized because, in contrast to the NMA-- $\text{Na}^+$  contact pair and the free aqueous NMA, the calcium ion replaces all the hydrogen bonding water molecules to the carbonyl as shown in Figure 4 which thus leads to an observable solvochromatic shifts.

In summary, this study presents a comprehensive investigation of cationic binding to the aqueous amide group using state-of-the-art *ab initio* molecular dynamics techniques in conjunction with rigorous statistical mechanics and spectra modelling. By means of umbrella sampling we construct free energy profiles for the interactions of  $\text{Na}^+$  and  $\text{Ca}^{2+}$  with aqueous NMA. Both free energy curves exhibit distinct contact and solvent shared pairs of the cations with the carbonyl group of NMA, but the binding of calcium to NMA is stronger than that of sodium. From the structural point of view, the most significant difference between the two cations is that calcium replaces all water molecules in the vicinity and binds to the amide carbonyl group collinearly. In contrast, the sodium ion only replaces a single water molecule and does not significantly alter the distribution of hydrogen bonding populations to the carbonyl oxygen, thus making it difficult to be detected via an IR shift. Compared to  $\text{Na}^+$ , the perturbation of the IR spectra due to  $\text{Ca}^{2+}$  binding is more significant because its solvation alters the hydrogen bond population of the carbonyl leading to a blue shift of the amide I band of about  $23\text{cm}^{-1}$ . These results are not only in good agreement with experiment, but also provide a detailed molecular picture of cationic interactions with the amide bond in water and the exquisite relationship of the ion binding to computed hydrogen bond populations and the observed IR spectra. The present study provides additional evidence that the rationalization of ion-specific Hofmeister effects on proteins requires accurate description of local interactions afforded here by quantum-based interaction potentials.

## COMPUTATIONAL DETAILS

We performed Born-Oppenheimer AIMD simulations at constant temperature (300 K) and volume, employing periodic boundary conditions using the Quickstep module of the CP2K package<sup>29</sup> with hybrid Gaussian and plane waves method (GPW) implemented<sup>30</sup>. The simulation cell consisted of the NMA molecule, 107 water molecules, and a single  $\text{Ca}^{2+}$  or  $\text{Na}^+$

ion in a cubic box with the edge length of 14.74 Å for the former or 14.96 Å for latter cation. The canonical sampling through velocity rescaling (CSVR) thermostat<sup>31</sup> with time constant of 50 fs was used to maintain the temperature of 300 K. The system was treated at the density functional level of theory employing the BLYP functional<sup>32, 33</sup> with the Grimme correction scheme<sup>34</sup> to account for dispersion interactions. Kohn-Sham orbitals were expanded in a Gaussian basis set (TZV2P MOLOPT for O, H, C, and N and DZVP-MOLOPT-SR-GTH-q10(9) for Ca(Na))<sup>30</sup>, while the core electrons were described by norm-conserving GTH pseudopotentials<sup>35</sup>. A cutoff of 400 Ry was used for the auxiliary plane wave basis set. The high exponent for the Na basis may require a higher cutoff for well converged forces. In order to justify our approach, we have checked the Na-O radial distribution functions with additional runs using a 600 Ry cutoff and found that they agree within error bars with results of simulations employing a 400 Ry cutoff.

The free energy profiles for the C=O···cation interaction were obtained by umbrella sampling. The initial conditions for AIMD simulations were taken from classical MD with the NMA and Na<sup>+</sup> empirical force field from our previous study<sup>13</sup>, OPLS<sup>13, 20</sup> force field for Ca<sup>2+</sup> and SPC/E<sup>36</sup> model for water. Sampling windows for the O···cation distance ranging from 2.5 to 6.5 Å were equally spaced by 0.5 Å employing harmonic umbrella potentials with a force constant of  $4 \cdot 10^3$  kJ mol<sup>-1</sup> nm<sup>-2</sup>. To ensure sufficient sampling in the barrier region, which is for both cation located around the O···cation distance of 3 Å, additional windows with stiffer force constants were added ( $8 \cdot 10^3$  kJ mol<sup>-1</sup> nm<sup>-2</sup> at 2.8 Å,  $1 \cdot 10^4$  kJ mol<sup>-1</sup> nm<sup>-2</sup> at 3.0 Å, and  $8 \cdot 10^3$  kJ mol<sup>-1</sup> nm<sup>-2</sup> at 3.3 Å). In each umbrella window a trajectory of at least 50 ps was collected after 5 ps of equilibration. The weighted histogram analysis method (WHAM)<sup>19</sup> was employed to extract a free energy profile from these histograms. A lower bound of the statistical error of the reported free energies is obtained from the WHAM procedure performed on collected BOMD histograms as  $\pm 0.5$  kJ/mol. However, one should keep in mind that this estimate is

inherently small once histograms reasonably overlap, but they may still be shifted with respect to perfect distributions from infinitely long simulation. A rough upper bound for the statistical error of  $\pm 2.5$  kJ/mol was, therefore, estimated from the standard deviations of the free energy profiles obtained from 50 ps pieces of a 10 ns classical MD trajectory in each umbrella sampling window.

For a direct comparison between experimentally observed shifts for the C=O stretch vibration (amide I band) vibrational spectra were calculated for aqueous NMA and NMA with  $\text{Ca}^{2+}$  or  $\text{Na}^+$  in its equilibrium position as a contact pair. To reproduce the experimental conditions, all acidic protons (on water and amine) were exchanged with deuterium. Five independent runs are started taking well equilibrated structures from runs started in the local minimum of the contact pair. After doubling the hydrogen mass, each system was initially equilibrated using massive thermostating in an NVT ensemble. For the calculation of vibrational spectra these were extended in the micro-canonical ensemble for 20 ps each. The IR spectra were calculated using the Fourier transforms of the dipole autocorrelation functions for the NMA molecule only. A harmonic quantum correction factor was applied and the resulting spectra were smoothed by a Gaussian convolution kernel of  $10 \text{ cm}^{-1}$  standard deviation.<sup>23</sup> The molecular dipoles were computed using the atomic core charges together with nearest Wannier function centers with a sampling frequency of 0.5 fs. To estimate the C-O stretch frequency, the power spectrum of the C-O bond length was calculated for windows of 4 ps using starting points 1 ps apart.

## SUPPORTING INFORMATION

Supporting information contains free energy profiles calculated using four empirical force fields and further testing of the free energy method. This material is available free of charge via the Internet at <http://pubs.acs.org>.

## ACKNOWLEDGMENT

Support from the Czech Ministry of Education (grant LH12001) is gratefully acknowledged. EP thanks the International Max-Planck Research School for support and acknowledges the Alternative Sponsored Fellowship program at Pacific Northwest National Laboratory (PNNL). PJ acknowledges the Praemium Academie award from the Academy of Sciences. Calculations of the free energy profiles were made possible through generous allocation of computer time from the North-German Supercomputing Alliance (HLRN). Calculations of vibrational spectra were performed in part using the computational resources in the National Energy Research Supercomputing Center (NERSC) at Lawrence Berkeley National Laboratory which is supported by the Office of Science of the U.S. Department of Energy under Contract No. DE-AC02-05CH11231. CJM is supported by the U.S. Department of Energy's (DOE) Office of Basic Energy Sciences, Division of Chemical Sciences, Geosciences and Biosciences. Pacific Northwest National Laboratory (PNNL) is operated for the Department of Energy by Battelle. MDB is grateful for the support of the Linus Pauling Distinguished Postdoctoral Fellowship Program at PNNL.

## REFERENCES

- (1) Nandi, P. K.; Robinson, D. R. Effects of Salts on Free-Energy of Peptide Group. *J. Am. Chem. Soc.* **1972**, *94*, 1299-1310.
- (2) Arakawa, T.; Timasheff, S. N. Mechanism of Protein Salting In and Salting Out by Divalent Cation Salts - Balance between Hydration and Salt Bridging. *Biochemistry* **1984**, *23*, 5912-5923.
- (3) Street, T. O.; Bolen, D. W.; Rose, G. D. A Molecular Mechanism for Msmolyte-Induced Protein Stability. *Proc. Nat. Acad. Sci. USA* **2006**, *103*, 17064-17064.
- (4) Collins, K. D.; Neilson, G. W.; Enderby, J. E. Ions in Water: Characterizing the Forces that Control Chemical Processes and Biological Structure. *Biophys. Chem.* **2007**, *128*, 95-104.
- (5) Zhang, Y. J.; Cremer, P. S. Chemistry of Hofmeister Anions and Osmolytes. *Ann. Rev. Phys. Chem.* **2010**, *61*, 63-83.
- (6) Pegram, L. M.; Record, M. T. Thermodynamic Origin of Hofmeister Ion Effects. *J. Phys. Chem. B* **2008**, *112*, 9428-9436.
- (7) Pluharova, E.; Marsalek, O.; Schmidt, B.; Jungwirth, P. Peptide Salt Bridge Stability: From Gas Phase via Microhydration to Bulk Water Simulations. *Journal of Chemical Physics* **2012**, *137*, 185101.
- (8) Paterova, J.; Rembert, K. B.; Heyda, J.; Kurra, Y.; Okur, H. I.; Liu, W. S. R.; Hilty, C.; Cremer, P. S.; Jungwirth, P. Reversal of the Hofmeister Series: Specific Ion Effects on Peptides. *J. Phys. Chem. B* **2013**, *117*, 8150-8158.
- (9) Horinek, D.; Moeser, B. Unified Description of Urea Denaturation: Backbone and Side Chains Contribute Equally in the Transfer Model. *J. Phys. Chem. B* **2014**, *118*, 107-114.
- (10) Pegram, L. M.; Record, M. T. Hofmeister Salt Effects on Surface Tension Arise from Partitioning of Anions and Cations between Bulk Water and the Air-Water Interface. *J. Phys. Chem. B* **2007**, *111*, 5411-5417.

- (11) Hladilkova, J.; Heyda, J.; Rembert, K. B.; Okur, H. I.; Kurra, Y.; Liu, W. S. R.; Hilty, C.; Cremer, P. S.; Jungwirth, P. Effects of End-Group Termination on Salting-Out Constants for Triglycine. *J. Phys. Chem. Lett.* **2013**, *4*, 4069-4073.
- (12) Okur, H. I.; Kherb, J.; Cremer, P. S. Cations Bind Only Weakly to Amides in Aqueous Solutions. *J. Am. Chem. Soc.* **2013**, *135*, 5062-5067.
- (13) Heyda, J.; Vincent, J. C.; Tobias, D. J.; Dzubiella, J.; Jungwirth, P. Ion Specificity at the Peptide Bond: Molecular Dynamics Simulations of N-Methylacetamide in Aqueous Salt Solutions. *J. Phys. Chem. B* **2010**, *114*, 1213-1220.
- (14) Algaer, E. A.; van der Vegt, N. F. A. Hofmeister Ion Interactions with Model Amide Compounds. *J. Phys. Chem. B* **2011**, *115*, 13781-13787.
- (15) Ganguly, P.; Schravendijk, P.; Hess, B.; van der Vegt, N. F. A. Ion Pairing in Aqueous Electrolyte Solutions with Biologically Relevant Anions. *J. Phys. Chem. B* **2011**, *115*, 3734-3739.
- (16) Pluharova, E.; Marsalek, O.; Schmidt, B.; Jungwirth, P. Ab Initio Molecular Dynamics Approach to a Quantitative Description of Ion Pairing in Water. *J. Phys. Chem. Lett.* **2013**, *4*, 4177-4181.
- (17) Smiechowski, M.; Forbert, H.; Marx, D. Spatial Decomposition and Assignment of Infrared Spectra of Simple Ions in Water from Mid-Infrared to THz Frequencies: Li+(aq) and F-(aq). *J. Chem. Phys.* **2013**, *139*, 014506
- (18) Allison, S. K.; Bates, S. P.; Crain, J.; Martyna, G. J. Solution Structure of the Aqueous Model Peptide N-Methylacetamide. *J. Phys. Chem. B* **2006**, *110*, 21319-21326.
- (19) Kumar, S.; Bouzida, D.; Swendsen, R. H.; Kollman, P. A.; Rosenberg, J. M. The Weighted Histogram Analysis Method for Free Energy Calculations on Biomolecule. 1. The Method. *J. Comp. Chem.* **1992**, *13*, 1011-1021.



- (20) Kaminski, G. A.; Friesner, R. A.; Tirado-Rives, J.; Jorgensen, W. L. Evaluation and Reparametrization of the OPLS-AA Force Field for Proteins via Comparison with Accurate Quantum Chemical Calculations on Peptides. *J. Phys. Chem. B* **2001**, *105*, 6474-6487.
- (21) Gaigeot, M. P.; Vuilleumier, R.; Sprik, M.; Borgis, D. Infrared Spectroscopy of N-Methylacetamide Revisited by Ab Initio Molecular Dynamics Simulations. *J. Chem. Theor. Comput.* **2005**, *1*, 772-789.
- (22) Gaigeot, M. P.; Martinez, M.; Vuilleumier, R. Infrared Spectroscopy in the Gas and Liquid Phase from First Principle Molecular Dynamics Simulations: Application to Small Peptides. *Mol. Phys.* **2007**, *105*, 2857-2878.
- (23) Mathias, G.; Baer, M. D. Generalized Normal Coordinates for the Vibrational Analysis of Molecular Dynamics Simulations. *J. Chem. Theor. Comput.* **2011**, *7*, 2028-2039.
- (24) VandeVondele, J.; Troster, P.; Tavan, P.; Mathias, G. Vibrational Spectra of Phosphate Ions in Aqueous Solution Probed by First-Principles Molecular Dynamics. *J. Phys. Chem. A* **2012**, *116*, 2466-2474.
- (25) Chen, X. G.; Schweitzerstener, R.; Asher, S. A.; Mirkin, N. G.; Krimm, S. Vibrational Assignments of Trans-N-Methylacetamide and Some of its Deuterated Isotopomers from Band Decomposition of IR, Visible, and Resonance Raman Spectra. *J. Phys. Chem.* **1995**, *99*, 3074-3083.
- (26) Kubelka, J.; Keiderling, T. A. Ab Initio Calculation of Amide Carbonyl Stretch Vibrational Frequencies in Solution with Modified Basis Sets. 1. N-Methyl Acetamide. *J. Phys. Chem. A* **2001**, *105*, 10922-10928.
- (27) Andrushchenko, V.; Matejka, P.; Anderson, D. T.; Kaminsky, J.; Hornicek, J.; Paulson, L. O.; Bour, P. Solvent Dependence of the N-Methylacetamide Structure and Force Field. *J. Phys. Chem. A* **2009**, *113*, 9727-9736.

- (28) Schmidt, J. R.; Corcelli, S. A.; Skinner, J. L. Ultrafast Vibrational Spectroscopy of Water and Aqueous N-methylacetamide: Comparison of Different Electronic Structure/Molecular Dynamics Approaches. *J. Chem. Phys.* **2004**, *121*, 8887-8896.
- (29) VandeVondele, J.; Krack, M.; Mohamed, F.; Parrinello, M.; Chassaing, T.; Hutter, J. QUICKSTEP: Fast and Accurate Density Functional Calculations Using a Mixed Gaussian and Plane Waves Approach. *Comp. Phys. Commun.* **2005**, *167*, 103-128.
- (30) VandeVondele, J.; Hutter, J. Gaussian Basis Sets for Accurate Calculations on Molecular Systems in Gas and Condensed Phases. *J. Chem. Phys.* **2007**, *127*, 114105.
- (31) Bussi, G.; Donadio, D.; Parrinello, M. Canonical Sampling through Velocity Rescaling. *J. Chem. Phys.* **2007**, *126*, 014101.
- (32) Becke, A. D. Density-Functional Exchange-Energy Approximation with Correct Asymptotic-Behavior. *Phys. Rev. A* **1988**, *38*, 3098-3100.
- (33) Lee, C. T.; Yang, W. T.; Parr, R. G. Development of the Colle-Salvetti Correlation-Energy Formula into a Functional of the Electron-Density. *Phys. Rev. B* **1988**, *37*, 785-789.
- (34) Grimme, S.; Antony, J.; Ehrlich, S.; Krieg, H. A Consistent and Accurate Ab Initio Parametrization of Density Functional Dispersion Correction (DFT-D) for the 94 Elements H-Pu. *J. Chem. Phys.* **2010**, *132*, 154104.
- (35) Goedecker, S.; Teter, M.; Hutter, J. Separable Dual-Space Gaussian Pseudopotentials. *Phys. Rev. B* **1996**, *54*, 1703-1710.
- (36) Berendsen, H. J. C.; Grigera, J. R.; Straatsma, T. P. The Missing Term in Effective Pair Potentials. *J. Phys. Chem.* **1987**, *91*, 6269-6271.